

SECOND ORDER REDUCED MODEL VIA INCREMENTAL PROJECTION FOR NAVIER STOKES

M. AZAÏEZ, Y. GUO, C. NÚÑEZ FERNÁNDEZ, S. RUBINO, AND C. XU

ABSTRACT. The numerical simulation of incompressible flows is challenging due to the tight coupling of velocity and pressure. Projection methods offer an effective solution by decoupling these variables, making them suitable for large-scale computations. This work focuses on reduced-order modeling using incremental projection schemes for the Stokes equations. We present both semi-discrete and fully discrete formulations, employing BDF2 in time and finite elements in space. A proper orthogonal decomposition (POD) approach is adopted to construct a reduced-order model for the Stokes problem. The method enables explicit computation of reduced velocity and pressure while preserving accuracy. We provide a detailed stability analysis and derive error estimates, showing second-order convergence in time. Numerical experiments are conducted to validate the theoretical results and demonstrate computational efficiency.

1. INTRODUCTION

Numerical simulation of incompressible flows presents a significant challenge due to the coupling of velocity and pressure imposed by the incompressibility constraint. Projection methods emerged in the late 1960s as a promising solution to this problem, pioneered by the groundbreaking work of Chorin and Temam [3, 18]. These methods are particularly appealing because they allow the decoupling of velocity and pressure computations at each time step, reducing the problem to a series of independent elliptic equations. This decoupling makes projection methods highly efficient for large-scale numerical simulations.

Although projection methods fall under the broader category of fractional or splitting step approaches, the standard methodologies for fractional step methods (e.g., Yanenko [19] or Glowinski [6], Chap. II) do not apply directly. This is because pressure is not a dynamic variable, and the Navier–Stokes equations do not conform to the Cauchy–Kovalevskaya form. Consequently, developing and analyzing higher-order projection methods has been a non-trivial task. Over the past years,

Date: December 12, 2025.

2010 Mathematics Subject Classification. 65N30.

Key words and phrases. Reduced order model; Stokes equation; Error estimate.

M. Azaïez: Bordeaux University, Bordeaux INP and I2M (UMR CNRS 5295), France. azaiez@u-bordeaux.fr.

Y. Guo: School of Mathematical Sciences and Fujian Provincial Key Laboratory of Mathematical Modeling and High Performance Scientific Computing, Xiamen University, 361005 Xiamen, China. yayuguo@stu.xmu.edu.cn.

C. Núñez Fernández: Departamento EDAN & IMUS, Universidad de Sevilla, Spain. cnfernandez@us.es.

S. Rubino: Departamento EDAN & IMUS, Universidad de Sevilla, Spain. samuele@us.es.

C. Xu: School of Mathematical Sciences and Fujian Provincial Key Laboratory of Mathematical Modeling and High Performance Scientific Computing, Xiamen University, 361005 Xiamen, China. cjxu@xmu.edu.cn.

extensive research has been conducted to construct, analyze, and refine projection schemes, with considerable effort devoted to finding optimal approaches (see, e.g., Glowinski [[6], Chap. VII]).

Although many valuable insights have been gained, the field has also had its share of erroneous or misleading claims. However, recent advances have addressed several long-standing theoretical and practical challenges, leading to a clearer understanding of projection methods. Recognizing this progress, Guermond and collaborators (see [9]) have compiled a comprehensive overview, presenting the best approximation results for various classes of projection schemes, and addressing critical implementation issues that are rarely discussed in the literature. Despite their advantages, relatively little research has focused on reduced-order methods using time-splitting techniques for unsteady Stokes or incompressible Navier-Stokes problems. Notable exceptions include the work of Li et al. [14], who proposed a reduced-order model (ROM) based on proper orthogonal decomposition (POD-ROM) for unsteady Stokes equations. Their approach combines the classical Chorin-Temam projection method with POD techniques, decoupling the reduced velocity and pressure variables. They circumvented the need to verify the classical LBB/inf-sup condition in mixed reduced spaces by using a stabilized pressure projection of the Petrov-Galerkin (PSPG) type. More recently, Azaiez et al. (see [1]) have presented a reduced-order method based on the Goda time-splitting scheme (standard incremental) [7], an improvement over the classical Chorin-Temam pressure correction method. Their approach computes POD pressure modes using an inner product that not only matches the pressure regularity in full-order finite element (FE) solutions, but also allows fully explicit computation for reduced velocity and pressure. This framework improves both consistency and computational efficiency.

In this paper, we propose to consider incremental projection methods to approximate the reduced-order Navier-Stokes equation (see [12]). The advantage of this method is the following, the error on the velocity in the semi-discret norme $L^2(L^2(\Omega)^d)$ (discret in time and continuous in space) is of $\mathcal{O}(\delta t^2 + h^{l+1})$, where $l \geq 1$ is the polynomial degree of the velocity approximation. One can read the proof in [12] where it is also shown that the splitting error of the projection schemes, based on the incremental pressure correction is $\mathcal{O}(\delta t^2)$ even if the application of the time derivative of the velocity is $\mathcal{O}(\delta t)$

The paper is devoted to the proposal of a reduced-order method to the incremental projection scheme. It is organised as follows : in Section 2, we give semi-discrete and fully discrete schemes respectively, using the BDF2 scheme in time and the finite element scheme in space. In section 3, we mainly introduce POD method and construct a reduced order model about Stokes equation. Meanwhile, we give the corresponding stability analysis and error estimation. In the last section, some numerical examples are calculated to verify the theoretical analysis.

2. SECOND ORDER INCREMENTAL SCHEME

The unsteady Stokes equation can be expressed as follows

$$\mathbf{u}_t - \nu \Delta \mathbf{u} + \nabla p = \mathbf{f}, \quad \text{in } \Omega \times]0, T], \quad (2.1a)$$

$$\nabla \cdot \mathbf{u} = 0, \quad \text{in } \Omega \times]0, T], \quad (2.1b)$$

$$\mathbf{u}|_{\partial\Omega} = 0, \quad \text{in }]0, T], \quad (2.1c)$$

$$\mathbf{u}|_{t=0} = \mathbf{u}^0, \quad \text{in } \Omega, \quad (2.1d)$$

where Ω is a bounded domain with a sufficiently smooth boundary $\partial\Omega$. \mathbf{u} denotes the velocity and p stands for the pressure.

We construct the second-order schemes in time, and use the finite element method in space.

2.1. Semi-discrete scheme. Let $\tau > 0$ be a time step and set $t^k = k\tau$ for $0 \leq k \leq N_t = [T/\tau]$.

Let us take a quick look at the scheme required for this article (See for more details [9, 12]).

We consider the two-step backward differentiation formula (BDF-2): for $n \geq 1$.

Step 1: Calculate $\tilde{\mathbf{u}}^{n+1}$ by

$$\frac{3\tilde{\mathbf{u}}^{n+1} - 4\mathbf{u}^n + \mathbf{u}^{n-1}}{2\tau} - \nu \Delta \tilde{\mathbf{u}}^{n+1} + \nabla p^n = \mathbf{f}^{n+1}, \quad (2.2a)$$

$$\tilde{\mathbf{u}}^{n+1}|_{\partial\Omega} = 0, \quad (2.2b)$$

Step 2: Compute ϕ^{n+1} by

$$\frac{3\mathbf{u}^{n+1} - 3\tilde{\mathbf{u}}^{n+1}}{2\tau} + \nabla \phi^{n+1} = 0, \quad (2.3a)$$

$$\nabla \cdot \mathbf{u}^{n+1} = 0, \quad (2.3b)$$

$$\mathbf{u}^{n+1} \cdot \mathbf{n} = 0, \quad (2.3c)$$

where we take $\phi^{n+1} = p^{n+1} - p^n$. From (2.3), we recover the velocity as

$$\mathbf{u}^{n+1} = \tilde{\mathbf{u}}^{n+1} - \frac{2}{3}\tau \nabla(p^{n+1} - p^n).$$

Similarly, at $t = t^n$ time step, we can derive

$$\mathbf{u}^n = \tilde{\mathbf{u}}^n - \frac{2}{3}\tau \nabla(p^n - p^{n-1}),$$

Meanwhile, we have the following result at t^{n-1} time step

$$\mathbf{u}^{n-1} = \tilde{\mathbf{u}}^{n-1} - \frac{2}{3}\tau \nabla(p^{n-1} - p^{n-2}).$$

Substituting the above equations into (2.2), and go to the Step 2, the final scheme is reformulated as

$$\frac{3\tilde{\mathbf{u}}^{n+1} - 4\tilde{\mathbf{u}}^n + \tilde{\mathbf{u}}^{n-1}}{2\tau} - \nu \Delta \tilde{\mathbf{u}}^{n+1} + \frac{1}{3}\nabla(7p^n - 5p^{n-1} + p^{n-2}) = \mathbf{f}^{n+1}, \quad (2.4a)$$

$$\tilde{\mathbf{u}}^{n+1}|_{\partial\Omega} = 0, \quad (2.4b)$$

For the second step, by using the divergence operator to the equation (2.3), which can be rewritten as

$$-\nabla \cdot \tilde{\mathbf{u}}^{n+1} + \frac{2\tau}{3} \Delta \phi^{n+1} = 0. \quad (2.5)$$

where $\phi^{n+1} = p^{n+1} - p^n$. So at the first step we compute $\tilde{\mathbf{u}}^{n+1}$, and then put it in scheme (2.5), we can get ϕ^{n+1} . Finally, update p^{n+1} by $p^{n+1} = \phi^{n+1} + p^n$.

2.2. Fully discrete scheme. Let $\mathcal{T}_h = \{K\}$ be the quasiuniform triangulation of Ω . Define the finite element spaces

$$U_h = \{\mathbf{v}_h \in X \cap C(\bar{\Omega})^2 : v_h|_K \in \mathcal{P}_2(K), \forall K \in \mathcal{T}_h\},$$

$$Q_h = \{q_h \in M : q_h|_K \in \mathcal{P}_1(K), \forall K \in \mathcal{T}_h\},$$

where $\mathcal{P}_1(K)$ is the space of polynomials of degree not exceeding 1. The fully discrete scheme is formulated as below: for $n \geq 1$, find $\tilde{\mathbf{u}}_h^{n+1} \in U_h$ and $p_h^{n+1} \in Q_h$, such that

$$\left(\frac{3\tilde{\mathbf{u}}_h^{n+1} - 4\tilde{\mathbf{u}}_h^n + \tilde{\mathbf{u}}_h^{n-1}}{2\tau}, \mathbf{v}_h \right) + \nu(\nabla \tilde{\mathbf{u}}_h^{n+1}, \nabla \mathbf{v}_h) + \frac{1}{3}(\nabla(7p_h^n - 5p_h^{n-1} + p_h^{n-2}), \mathbf{v}_h) = (f^{n+1}, \mathbf{v}_h), \quad \forall \mathbf{v}_h \in U_h, \quad (2.6a)$$

$$(\nabla \cdot \tilde{\mathbf{u}}_h^{n+1}, q_h) + \frac{2\tau}{3}(\nabla \phi_h^{n+1}, \nabla q_h) = 0, \quad \forall q_h \in Q_h, \quad (2.6b)$$

then we update $p_h^{n+1} = \phi_h^{n+1} + p_h^n$. Here we compute $\tilde{\mathbf{u}}_h^1, \tilde{\mathbf{u}}_h^2$ and p_h^1, p_h^2 by first order scheme.

3. THE POD REDUCED ORDER MODEL

In this section, we introduce the POD method briefly. This method can save computing costs by replacing global basis functions with reduced basis. The detailed presentation can be referred to [13].

3.1. The proper orthogonal decomposition. Define \mathcal{V} and \mathcal{P} are ensembles of snapshots, i.e. $\mathcal{V} = \text{span}\{\tilde{\mathbf{u}}_1, \tilde{\mathbf{u}}_2, \dots, \tilde{\mathbf{u}}_{N_t+1}\}$, $\mathcal{P} = \text{span}\{p_1, p_2, \dots, p_{N_t+1}\}$ where $\tilde{\mathbf{u}}_i = \tilde{\mathbf{u}}_h^{i-1}(x, y)$ ($1 \leq i \leq N_t + 1$), $p_i = p_h^{i-1}(x, y)$ ($1 \leq i \leq N_t + 1$). The goal of the POD method is to seek two orthogonal bases $\{\varphi_1, \varphi_2, \dots, \varphi_{N_u}\}$, $\{\psi_1, \psi_2, \dots, \psi_{N_p}\}$ to optimize the following minimization problems

$$\min_{\{\phi_j\}_{j=1}^{N_u}} \frac{1}{N_t + 1} \sum_{i=1}^{N_t+1} \left\| \tilde{\mathbf{u}}_i - \sum_{j=1}^{N_u} (\tilde{\mathbf{u}}_i, \varphi_j)_X \varphi_j \right\|_X^2, \quad (3.1)$$

$$\min_{\{\psi_j\}_{j=1}^{N_p}} \frac{1}{N_t + 1} \sum_{i=1}^{N_t+1} \left\| p_i - \sum_{j=1}^{N_p} (p_i, \psi_j)_Y \psi_j \right\|_Y^2, \quad (3.2)$$

subject to $(\varphi_i, \varphi_j)_X = (\nabla \varphi_i, \nabla \varphi_j) = \delta_{ij}$, $1 \leq i, j \leq N_u$ and $(\psi_i, \psi_j)_Y = (\nabla \psi_i, \nabla \psi_j) = \delta_{ij}$, $1 \leq i, j \leq N_p$, where δ_{ij} is the Kronecker delta. The solutions of (3.1) and (3.2) are given by the solving the eigenvalue problem:

$$\mathcal{K}^{\mathbf{u}} \tilde{\varphi}_i = \lambda_i \tilde{\varphi}_i, \quad i = 1, 2, \dots, N_t + 1,$$

$$\mathcal{K}^p \tilde{\psi}_i = \lambda_i \tilde{\psi}_i, \quad i = 1, 2, \dots, N_t + 1,$$

in which $\mathcal{K}^{\mathbf{u}} = (K_{ij}^{\mathbf{u}})_{N_t+1, N_t+1} \in R^{(N_t+1) \times (N_t+1)}$ and $\mathcal{K}^p = (K_{ij}^p)_{N_t+1, N_t+1} \in R^{(N_t+1) \times (N_t+1)}$ denote the correlation matrixs, where $K_{ij}^{\mathbf{u}} = \frac{1}{N_t+1}(\nabla \tilde{\mathbf{u}}_i, \nabla \tilde{\mathbf{u}}_j)$, $K_{ij}^p = \frac{1}{N_t+1}(\nabla p_i, \nabla p_j)$, $\tilde{\phi}_i$ and $\tilde{\psi}_i$ are the eigenvector corresponding to the eigenvalue λ_i and σ_i respectively, and $\lambda_1 \geq \lambda_2 \geq \dots \geq \lambda_{N_t+1} \geq 0$, σ_i . Furthermore, the POD basis functions of rank $N_u, N_p \leq N_t + 1$ are given by the formula

$$\varphi_i = \frac{1}{\sqrt{(N_t+1)\lambda_i}} \sum_{k=0}^{N_t+1} (\tilde{\varphi}_i)_k \tilde{\mathbf{u}}_k, \quad i = 1, 2, \dots, N_u,$$

$$\psi_i = \frac{1}{\sqrt{(N_t+1)\sigma_i}} \sum_{k=0}^{N_t+1} (\tilde{\psi}_i)_k p_k, \quad i = 1, 2, \dots, N_p,$$

where $(\tilde{\varphi}_i)_k$ and $(\tilde{\psi}_i)_k$ denote the k -th component of $\tilde{\varphi}_i$ and $\tilde{\psi}_i$, respectively. Then the errors of POD method are given by

$$\frac{1}{N_t+1} \sum_{i=1}^{N_t+1} \|\tilde{\mathbf{u}}_i - \sum_{j=1}^{N_u} (\tilde{\mathbf{u}}_i, \varphi_j)_X \varphi_j\|_X^2 = \sum_{j=N_u+1}^{N_t+1} \lambda_j,$$

$$\frac{1}{N_t+1} \sum_{i=1}^{N_t+1} \|p_i - \sum_{j=1}^{N_p} (p_i, \psi_j)_Y \psi_j\|_Y^2 = \sum_{j=N_p+1}^{N_t+1} \sigma_j.$$

Then we construct the reduce model for unsteady stokes by using the POD basis.

3.2. Formulating projection ROM. Let

$$U_r = \{\varphi_1, \varphi_2, \dots, \varphi_{N_u}\},$$

$$Q_r = \{\psi_1, \psi_2, \dots, \psi_{N_p}\},$$

A reduced order approximation of both FE-ROM velocity $\tilde{\mathbf{u}}_r^{n+1} \in U_r$ and pressure field $p_r^{n+1} \in Q_r$ such that

$$\frac{3\tilde{\mathbf{u}}_r^{n+1} - 4\tilde{\mathbf{u}}_r^n + \tilde{\mathbf{u}}_r^{n-1}}{2\tau} - \nu \Delta \tilde{\mathbf{u}}_r^{n+1} + \frac{1}{3} \nabla (7p_r^n - 5p_r^{n-1} + p_r^{n-2}) = f^{n+1}, \quad \text{in } \Omega, \quad (3.3a)$$

$$-\nabla \cdot \tilde{\mathbf{u}}_r^{n+1} + \frac{2\tau}{3} \Delta p_r^{n+1} = \frac{2\tau}{3} \Delta p_r^n, \quad \text{in } \Omega. \quad (3.3b)$$

Below we give the matrix calculation form. We first expand $\tilde{\mathbf{u}}_r, p_r$ by POD basis $\phi_i(\mathbf{x}), \psi_i(\mathbf{x})$ respectively

$$\tilde{\mathbf{u}}_r(\mathbf{x}, t) = \sum_{i=1}^{N_u} a_i(t) \varphi_i(\mathbf{x}),$$

$$p_r(\mathbf{x}, t) = \sum_{i=1}^{N_p} b_i(t) \psi_i(\mathbf{x}).$$

Substituting the above equations to (3.3) under the Galerkin framework, we obtain

$$\begin{aligned} \left(\frac{3\tilde{\mathbf{u}}_r^{n+1} - 4\tilde{\mathbf{u}}_r^n + \tilde{\mathbf{u}}_r^{n-1}}{2\tau}, \mathbf{v}_r \right) + \nu(\nabla \tilde{\mathbf{u}}_r^{n+1}, \mathbf{v}_r) \\ - \frac{1}{3}(7p_r^n - 5p_r^{n-1} + p_r^{n-2}, \nabla \cdot \mathbf{v}_r) = (f^{n+1}, \mathbf{v}_r), \quad \forall \mathbf{v}_r \in U_r, \end{aligned} \quad (3.4a)$$

$$(\nabla \cdot \tilde{\mathbf{u}}_r^{n+1}, q_r) + \frac{2\tau}{3}(\nabla p_r^{n+1}, \nabla q_r) = \frac{2\tau}{3}(\nabla p_r^n, \nabla q_r), \quad \forall q_r \in Q_r. \quad (3.4b)$$

Here we choose the test functions $\mathbf{v}_r = \varphi_i(\mathbf{x}), i = 1, \dots, N_u$, $q_r = \psi_j(\mathbf{x}), j = 1, \dots, N_p$, the following reduced system is obtained:

$$\left(\frac{3}{2\tau} \mathbf{M}_r + \mathbf{S}_r^u \right) \mathbf{a}^{n+1} = \frac{1}{2\tau} \mathbf{M}_r (4\mathbf{a}^n - \mathbf{a}^{n-1}) + \frac{1}{3} \mathbf{P} (7\mathbf{b}^n - 5\mathbf{b}^{n-1} + \mathbf{b}^{n-2}) + \mathbf{F}_r, \quad (3.5a)$$

$$\mathbf{S}_r^p \mathbf{b}^{n+1} = \mathbf{S}_r^p \mathbf{b}^n - \frac{3}{2\tau} \mathbf{P}^T \mathbf{a}^{n+1}. \quad (3.5b)$$

The matrices $\mathbf{M}_r \in R^{N_u \times N_u}$, $\mathbf{S}_r^u \in R^{N_u \times N_u}$, $\mathbf{F}_r \in R^{N_u \times 1}$, $\mathbf{P} \in R^{N_u \times N_p}$, $\mathbf{S}_r^p \in R^{N_p \times N_p}$ appearing in the system are defined as follows:

$$\begin{aligned} (\mathbf{M}_r)_{ij} &= (\varphi_i, \varphi_j), \quad (\mathbf{S}_r^u)_{ij} = (\nabla \varphi_i, \nabla \varphi_j), \quad (\mathbf{F})_{ij} = (f, \varphi_j), \\ (\mathbf{P})_{ij} &= (\psi_i, \nabla \cdot \varphi_j), \quad (\mathbf{S}_r^p)_{ij} = (\nabla \psi_i, \nabla \psi_j). \end{aligned}$$

3.3. Stability and error estimate of pressure projection ROM. Firstly, we prove that the algorithm (3.4) is stable.

Theorem 3.1. *The solution $\{(\tilde{\mathbf{u}}_r^n, p_r^n)\}$ to (3.4) satisfies the following estimates: for $\forall n \geq 2$*

$$\begin{aligned} \|\tilde{\mathbf{u}}_r^n\|_0^2 + \tau^2 \|\nabla p_r^n\|_0^2 + \tau^2 \|\nabla(p_r^{n-1} - p_r^{n-2})\|_0^2 + \sum_{k=2}^{N_t} (\nu \tau \|\nabla \tilde{\mathbf{u}}_r^k\|_0^2 + \tau^2 \|\nabla(p_r^{k-1} - p_r^{k-2})\|_0^2) \\ \leq c(\|\tilde{\mathbf{u}}_r^0\|_0^2 + \|\tilde{\mathbf{u}}_r^1\|_0^2 + \tau^2 \|\nabla p_r^0\|_0^2 + \tau^2 \|\nabla p_r^1\|_0^2 + \nu^{-1} \sum_{k=2}^{N_t} \tau \|f^k\|_{\mathbf{H}^{-1}}^2). \end{aligned} \quad (3.6)$$

Proof. Following the idea of [8], we can derive the stability of scheme (3.4). For the reader to read, we briefly describe the following. When $n = 1$ or 2 , we set $\mathbf{v}_r = 4\tau \tilde{\mathbf{u}}_r^{n+1}$ in (3.4). Using the identity

$$2a(3a - 4b + c) = a^2 + (2a - b)^2 + (a - 2b + c)^2 - b^2 - (2b - c)^2,$$

and Cauchy-Schwarz inequality we obtain

$$\begin{aligned} &\|\tilde{\mathbf{u}}_r^{n+1}\|_0^2 + \|2\tilde{\mathbf{u}}_r^{n+1} - \tilde{\mathbf{u}}_r^n\|_0^2 + \|\tilde{\mathbf{u}}_r^{n+1} - 2\tilde{\mathbf{u}}_r^n + \tilde{\mathbf{u}}_r^{n-1}\|_0^2 + 2\nu\tau \|\nabla \tilde{\mathbf{u}}_r^{n+1}\|_0^2 \\ &\leq \|\tilde{\mathbf{u}}_r^n\|_0^2 + \|2\tilde{\mathbf{u}}_r^n - \tilde{\mathbf{u}}_r^{n-1}\|_0^2 - \frac{4\tau^2}{3}(\nabla(7p_r^n - 5p_r^{n-1} + p_r^{n-2}), \tilde{\mathbf{u}}_r^{n+1}) + 2\nu^{-1}\tau \|f^{n+1}\|_{\mathbf{H}^{-1}}^2 \\ &\leq \|\tilde{\mathbf{u}}_r^n\|_0^2 + \|2\tilde{\mathbf{u}}_r^n - \tilde{\mathbf{u}}_r^{n-1}\|_0^2 + \frac{4\tau^2}{6} \|\nabla(7p_r^n - 5p_r^{n-1} + p_r^{n-2})\|_0^2 + \frac{1}{2} \|\tilde{\mathbf{u}}_r^{n+1}\|_0^2 + 2\nu^{-1}\tau \|f^{n+1}\|_{\mathbf{H}^{-1}}^2. \end{aligned}$$

The above inequality can be simplified as

$$\begin{aligned} & \frac{1}{2} \|\tilde{\mathbf{u}}_r^{n+1}\|_0^2 + \|\tilde{\mathbf{u}}_r^{n+1} - 2\tilde{\mathbf{u}}_r^n + \tilde{\mathbf{u}}_r^{n-1}\|_0^2 + 2\tau\nu \|\nabla \tilde{\mathbf{u}}_r^{n+1}\|_0^2 \\ & \leq \|\tilde{\mathbf{u}}_r^0\|_0^2 + \|\tilde{\mathbf{u}}_r^1\|_0^2 + \frac{4\tau^2}{3} \|\nabla(7p_r^n - 5p_r^{n-1} + p_r^{n-2})\|_0^2 + 2\nu^{-1}\tau \|f^{n+1}\|_{\mathbf{H}^{-1}}^2 \\ & \leq c(\|\tilde{\mathbf{u}}_r^0\|_0^2 + \|\tilde{\mathbf{u}}_r^1\|_0^2 + \tau^2 \|\nabla p_r^1\|_0^2 + \tau^2 \|\nabla p_r^0\|_0^2 + \nu^{-1}\tau \|f^{n+1}\|_{\mathbf{H}^{-1}}^2) \end{aligned} \quad (3.7)$$

for $n = 1$ or 2 . Then we derive the estimates of pressure. From (3.4b), the inequality holds

$$\frac{4\tau^2}{9} \|\nabla(p_r^{n+1} - p_r^n)\|_0^2 \leq \|\tilde{\mathbf{u}}_r^{n+1}\|_0^2. \quad (3.8)$$

Therefore, the estimates (3.6) obtained for $n = 1$ and 2 by combining the results (3.7) with (3.8). For $n \geq 3$, taking $\mathbf{v}_r = 4\tau\tilde{\mathbf{u}}_r^{n+1}$ in (3.4) and using the identity

$$2a(3a - 4b + c) = 3a^2 - 4b^2 + c^2 + 2(a - b)^2 - 2(b - c)^2 + (a - 2b + c)^2,$$

so we have

$$\begin{aligned} & 3\|\tilde{\mathbf{u}}_r^{n+1}\|_0^2 - 4\|\tilde{\mathbf{u}}_r^n\|_0^2 + \|\tilde{\mathbf{u}}_r^{n-1}\|_0^2 + 2\|\tilde{\mathbf{u}}_r^{n+1} - \tilde{\mathbf{u}}_r^n\|_0^2 - 2\|\tilde{\mathbf{u}}_r^n - \tilde{\mathbf{u}}_r^{n-1}\|_0^2 \\ & + \|\tilde{\mathbf{u}}_r^{n+1} - 2\tilde{\mathbf{u}}_r^n + \tilde{\mathbf{u}}_r^{n-1}\|_0^2 + 4\tau\nu \|\nabla \tilde{\mathbf{u}}_r^{n+1}\|_0^2 + 4\tau(\nabla p_r^{n+1}, \tilde{\mathbf{u}}_r^{n+1}) \\ & - 4\tau(\nabla(p_r^{n+1} - 2p_r^n + p_r^{n-1}), \tilde{\mathbf{u}}_r^{n+1}) + \frac{4\tau}{3}(\nabla(p_r^n - 2p_r^{n-1} + p_r^{n-2}), \tilde{\mathbf{u}}_r^{n+1}) = 4\tau\langle f^{n+1}, \tilde{\mathbf{u}}_r^{n+1} \rangle. \end{aligned} \quad (3.9)$$

Choosing $q_r = p_r^{n+1}$, $p_r^{n+1} - 2p_r^n + p_r^{n-1}$ and $p_r^n - 2p_r^{n-1} + p_r^{n-2}$ in (3.4b) respectively, the results lists as below

$$\begin{aligned} (\tilde{\mathbf{u}}_r^{n+1}, \nabla p_r^{n+1}) &= \frac{2\tau}{3}(\nabla(p_r^{n+1} - p_r^n), \nabla p_r^{n+1}) \\ &= \frac{\tau}{3}(\|\nabla p_r^{n+1}\|_0^2 - \|\nabla p_r^n\|_0^2 + \|\nabla(p_r^{n+1} - p_r^n)\|_0^2), \end{aligned} \quad (3.10)$$

$$\begin{aligned} (\tilde{\mathbf{u}}_r^{n+1}, \nabla(p_r^{n+1} - 2p_r^n + p_r^{n-1})) &= \frac{2\tau}{3}(\nabla(p_r^{n+1} - p_r^n), \nabla(p_r^{n+1} - 2p_r^n + p_r^{n-1})) \\ &= \frac{\tau}{3}(\|\nabla(p_r^{n+1} - p_r^n)\|_0^2 - \|\nabla(p_r^n - p_r^{n-1})\|_0^2 + \|\nabla(p_r^{n+1} - 2p_r^n + p_r^{n-1})\|_0^2), \end{aligned} \quad (3.11)$$

$$(\tilde{\mathbf{u}}_r^{n+1}, \nabla(p_r^n - 2p_r^{n-1} + p_r^{n-2})) = \frac{2\tau}{3}(\nabla(p_r^{n+1} - p_r^n), \nabla(p_r^n - 2p_r^{n-1} + p_r^{n-2})). \quad (3.12)$$

Putting (3.10)-(3.12) into (3.9) to get

$$\begin{aligned} & 3\|\tilde{\mathbf{u}}_r^{n+1}\|_0^2 - 4\|\tilde{\mathbf{u}}_r^n\|_0^2 + \|\tilde{\mathbf{u}}_r^{n-1}\|_0^2 + 2\|\tilde{\mathbf{u}}_r^{n+1} - \tilde{\mathbf{u}}_r^n\|_0^2 - 2\|\tilde{\mathbf{u}}_r^n - \tilde{\mathbf{u}}_r^{n-1}\|_0^2 \\ & + \|\tilde{\mathbf{u}}_r^{n+1} - 2\tilde{\mathbf{u}}_r^n + \tilde{\mathbf{u}}_r^{n-1}\|_0^2 + 4\tau\|\nabla \tilde{\mathbf{u}}_r^{n+1}\|_0^2 + \frac{4\tau^2}{3}(\|\nabla p_r^{n+1}\|_0^2 - \|\nabla p_r^n\|_0^2 \\ & + \|\nabla(p_r^n - p_r^{n-1})\|_0^2 - \|\nabla(p_r^{n+1} - 2p_r^n + p_r^{n-1})\|_0^2) \\ & + \frac{8\tau^2}{9}(\nabla(p_r^{n+1} - p_r^n), \nabla(p_r^n - 2p_r^{n-1} + p_r^{n-2})) = 4\tau\langle f^{n+1}, \tilde{\mathbf{u}}_r^{n+1} \rangle. \end{aligned} \quad (3.13)$$

Now we deal with the last term on the right hand of (3.13). Take the difference at time t^{n+1} and t^n of (3.4b), we derive

$$(\tilde{\mathbf{u}}_r^{n+1} - \tilde{\mathbf{u}}_r^n, \nabla q_r^n) = \frac{2\tau}{3}(\nabla(p_r^{n+1} - 2p_r^n + p_r^{n-1}), \nabla q_r). \quad (3.14)$$

Taking $q_r = \frac{2\tau}{3}(p_r^{n+1} - 2p_r^n + p_r^{n-1})$ in the above equation, we deduce that

$$(\tilde{\mathbf{u}}_r^{n+1} - \tilde{\mathbf{u}}_r^n, \nabla(p_r^{n+1} - 2p_r^n + p_r^{n-1})) = \frac{4\tau^2}{9} \|\nabla(p_r^{n+1} - 2p_r^n + p_r^{n-1})\|_0^2. \quad (3.15)$$

Using the equation $(a - b)^2 = a^2 - 2ab + b^2$, the above equation can be rewritten as

$$\|\tilde{\mathbf{u}}_r^{n+1} - \tilde{\mathbf{u}}_r^n\|_0^2 = \|\tilde{\mathbf{u}}_r^{n+1} - \tilde{\mathbf{u}}_r^n - \frac{2\tau}{3}\nabla(p_r^{n+1} - 2p_r^n + p_r^{n-1})\|_0^2 + \frac{4\tau^2}{9} \|\nabla(p_r^{n+1} - 2p_r^n + p_r^{n-1})\|_0^2. \quad (3.16)$$

Substituting (3.16) to (3.13) to obtain

$$\begin{aligned} & 3\|\tilde{\mathbf{u}}_r^{n+1}\|_0^2 - 4\|\tilde{\mathbf{u}}_r^n\|_0^2 + \|\tilde{\mathbf{u}}_r^{n-1}\|_0^2 + 2\|\tilde{\mathbf{u}}_r^{n+1} - \tilde{\mathbf{u}}_r^n - \frac{2\tau}{3}\nabla(p_r^{n+1} - 2p_r^n + p_r^{n-1})\|_0^2 \\ & - 2\|\tilde{\mathbf{u}}_r^n - \tilde{\mathbf{u}}_r^{n-1} - \frac{2\tau}{3}\nabla(p_r^n - 2p_r^{n-1} + p_r^{n-2})\|_0^2 + \|\tilde{\mathbf{u}}_r^{n+1} - 2\tilde{\mathbf{u}}_r^n + \tilde{\mathbf{u}}_r^{n-1}\|_0^2 \\ & + 4\tau\nu\|\nabla\tilde{\mathbf{u}}_r^{n+1}\|_0^2 + \frac{4\tau^2}{3}(\|\nabla p_r^{n+1}\|_0^2 - \|\nabla p_r^n\|_0^2 + \|\nabla(p_r^n - p_r^{n-1})\|_0^2) \\ & - \frac{4\tau^2}{9}\|\nabla(p_r^{n+1} - 2p_r^n + p_r^{n-1})\|_0^2 - \frac{8\tau^2}{9}\|\nabla(p_r^n - 2p_r^{n-1} + p_r^{n-2})\|_0^2 \\ & + \frac{8\tau^2}{9}(\nabla(p_r^{n+1} - p_r^n), \nabla(p_r^n - 2p_r^{n-1} + p_r^{n-2})) = 4\langle f^{n+1}, \tilde{\mathbf{u}}_r^{n+1} \rangle. \end{aligned} \quad (3.17)$$

Now we consider the last three terms on the right hand term of (3.17).

$$\begin{aligned} & -\frac{4\tau^2}{9}\|\nabla(p_r^{n+1} - 2p_r^n + p_r^{n-1})\|_0^2 - \frac{8\tau^2}{9}\|\nabla(p_r^n - 2p_r^{n-1} + p_r^{n-2})\|_0^2 \\ & + \frac{8\tau^2}{9}(\nabla(p_r^{n+1} - p_r^n), \nabla(p_r^n - 2p_r^{n-1} + p_r^{n-2})) \\ & = -\frac{4\tau^2}{9}\|\nabla(p_r^{n+1} - 3p_r^n + 3p_r^{n-1} - p_r^{n-2})\|_0^2 - \frac{4\tau^2}{9}(\nabla(p_r^n - 2p_r^{n-1} + p_r^{n-2}), \nabla(-p_r^n + p_r^{n-2})) \\ & = -\frac{4\tau^2}{9}\|\nabla(p_r^{n+1} - 3p_r^n + 3p_r^{n-1} - p_r^{n-2})\|_0^2 + \frac{4\tau^2}{9}(\nabla(p_r^n - 2p_r^{n-1} + p_r^{n-2}), \nabla((p_r^n - p_r^{n-1}) + (p_r^{n-1} - p_r^{n-2}))). \end{aligned}$$

Like as (3.8), we have

$$\frac{4\tau^2}{9}\|\nabla(p_r^{n+1} - 3p_r^n + 3p_r^{n-1} - p_r^{n-2})\|_0^2 \leq \|\tilde{\mathbf{u}}_r^{n+1} - 2\tilde{\mathbf{u}}_r^n + \tilde{\mathbf{u}}_r^{n-1}\|_0^2. \quad (3.18)$$

Then we have

$$\begin{aligned} & -\frac{4\tau^2}{9}\|\nabla(p_r^{n+1} - 2p_r^n + p_r^{n-1})\|_0^2 - \frac{8\tau^2}{9}\|\nabla(p_r^n - 2p_r^{n-1} + p_r^{n-2})\|_0^2 \\ & + \frac{8\tau^2}{9}(\nabla(p_r^{n+1} - p_r^n), \nabla(p_r^n - 2p_r^{n-1} + p_r^{n-2})) \\ & \geq -\|\tilde{\mathbf{u}}_r^{n+1} - 2\tilde{\mathbf{u}}_r^n + \tilde{\mathbf{u}}_r^{n-1}\|_0^2 + \frac{4\tau^2}{9}(\|\nabla(p_r^n - p_r^{n-1})\|_0^2 - \|\nabla(p_r^{n-1} - p_r^{n-2})\|_0^2). \end{aligned} \quad (3.19)$$

Furthermore, together all results, we can deduce the following estimate

$$\begin{aligned}
& 3\|\tilde{\mathbf{u}}_r^{n+1}\|_0^2 - 4\|\tilde{\mathbf{u}}_r^n\|_0^2 + \|\tilde{\mathbf{u}}_r^{n-1}\|_0^2 + 2\|\tilde{\mathbf{u}}_r^{n+1} - \tilde{\mathbf{u}}_r^n - \frac{2\tau}{3}\nabla(p_r^{n+1} - 2p_r^n + p_r^{n-1})\|_0^2 \\
& - 2\|\tilde{\mathbf{u}}_r^n - \tilde{\mathbf{u}}_r^{n-1} - \frac{2\tau}{3}\nabla(p_r^n - 2p_r^{n-1} + p_r^{n-2})\|_0^2 + 2\tau\nu\|\nabla\tilde{\mathbf{u}}_r^{n+1}\|_0^2 \\
& + \frac{4\tau^2}{3}(\|\nabla p_r^{n+1}\|_0^2 - \|\nabla p_r^n\|_0^2 + \|\nabla(p_r^n - p_r^{n-1})\|_0^2) \\
& + \frac{4\tau^2}{9}(\|\nabla(p_r^n - p_r^{n-1})\|_0^2 - \|\nabla(p_r^{n-1} - p_r^{n-2})\|_0^2) - 2\tau\nu^{-1}\|f^{n+1}\|_{\mathbf{H}^{-1}}^2 \leq 0.
\end{aligned} \tag{3.20}$$

Here we denote

$$\begin{aligned}
a^{k+1} &= \|\tilde{\mathbf{u}}_r^{n+1}\|_0^2, \\
b^{k+1} &= 2\tau\|\nabla\tilde{\mathbf{u}}_r^{n+1}\|_0^2 + \frac{4\tau^2}{3}\|\nabla(p_r^n - p_r^{n-1})\|_0^2 - 2\tau\nu^{-1}\|f^{n+1}\|_{\mathbf{H}^{-1}}^2, \\
d^{k+1} &= 2\|\tilde{\mathbf{u}}_r^{n+1} - \tilde{\mathbf{u}}_r^n - \frac{2\tau}{3}\nabla(p_r^{n+1} - 2p_r^n + p_r^{n-1})\|_0^2 + \frac{4\tau^2}{3}\|\nabla p_r^{n+1}\|_0^2 + \frac{4\tau^2}{9}\|\nabla(p_r^n - p_r^{n-1})\|_0^2.
\end{aligned}$$

Using the inequality of three term recursion appeared in [8] (Corollary 5.1), let $\{a^k\}_{k \geq 1}$ be the solution to the three term recursion inequality

$$3a^{k+1} - 4a^k + a^{k-1} \leq g^{k+1}, \tag{3.21}$$

with the initial condition a^0 and a^1 , where $g^{k+1} = -(b^{k+1} + d^{k+1} - d^k)$. Then the following estimate holds

$$a^\nu + \frac{1}{3}d^\nu + \frac{1}{3}\sum_{s=2}^\nu b^s \leq c(a^1 + a^2 + d^2), \tag{3.22}$$

where $c \in \mathbb{R}$. Finally, we omit some positive terms, then conclude the result (3.6). \square

We now claim the error analysis as follows. Define $\Pi_v : W_u(\Omega) \rightarrow U_r$ and $\Pi_q : W_p(\Omega) \rightarrow Q_r$ such that

$$\begin{aligned}
& ((\mathbf{u} - \Pi_v \mathbf{u}), \mathbf{v})_{W_u} = 0, \quad (\mathbf{u} - \Pi_v \mathbf{u}, 1) = 0, \quad \mathbf{v} \in U_r, \\
& ((p - \Pi_q p), q)_{W_p} = 0, \quad (p - \Pi_q p, 1) = 0, \quad q \in Q_r.
\end{aligned}$$

From the estimate of POD error, we have

$$\begin{aligned}
\frac{1}{N_t + 1} \sum_{i=1}^{N_t+1} \|\tilde{\mathbf{u}}_i - \Pi_v \tilde{\mathbf{u}}_i\|_{W_u}^2 &= \sum_{j=N_u+1}^{N_t+1} \lambda_j, \\
\frac{1}{N_t + 1} \sum_{i=1}^{N_t+1} \|p_i - \Pi_q p_i\|_{W_p}^2 &= \sum_{j=N_p+1}^{N_t+1} \sigma_j.
\end{aligned}$$

Note that we define a general space for build both reduced spaces, velocity and pressure respectively.

Before state the error estimation theorem, we need to define the following results:

Definition 3.1. Let X be a Hilbert space and Y, Z two finite-dimensional subspaces of X with intersection reduced to the zero function. The pair of finite-dimensional spaces (Y, Z) is called to satisfy the saturation property if there exists a positive constant C such that:

$$\|y\|_X + \|z\|_X \leq C\|y + z\|_X \quad \forall y \in Y, z \in Z. \quad (3.23)$$

The saturation property can be viewed as an inverse triangular inequality.

Lemma 3.1. (see [17], Lemma 5.3). The saturation property is equivalent to the existence of a constant $\alpha < 1$ such that:

$$|(y, z)_X| \leq \alpha\|y\|_X\|z\|_X \quad \forall y \in Y, z \in Z. \quad (3.24)$$

We will denote by α the saturation constant. Then, we can interpret the saturation property in the sense that the angle between spaces Y and Z , defined by:

$$\theta = \arccos \left(\sup_{y \in Y \setminus \{0\}, z \in Z \setminus \{0\}} \frac{(y, z)_X}{\|y\|_X\|z\|_X} \right), \quad (3.25)$$

is uniformly bounded from below by a positive angle, and $\alpha = \cos(\theta)$.

Remark 3.1. In the following error estimation theorem we will use the Lemma 3.1 to bound some of the error pressure terms.

Theorem 3.2. Let $\{(\tilde{\mathbf{u}}_r^n, p_r^n)\}$ and $\{(\tilde{\mathbf{u}}_h^n, p_h^n)\}$ be the solution of the problems (3.4) and (2.6). If the saturation constant α of Lemma 3.1 verifies $\alpha < 3/8$, then the following estimate holds: for $\forall n \geq 2$

$$\begin{aligned} & \sum_{n=1}^{N_t} \tau \|\tilde{\mathbf{u}}_r^{n+1} - \tilde{\mathbf{u}}_h^{n+1}\|_0^2 + 2\nu \sum_{n=1}^{N_t} \tau \|\nabla(\tilde{\mathbf{u}}_r^{n+1} - \tilde{\mathbf{u}}_h^{n+1})\|_0^2 + \frac{4\tau^2}{3} \sum_{n=1}^{N_t} \tau \|\nabla(p_r^{n+1} - p_h^{n+1})\|_0^2 \\ & \leq C(\alpha) e^{T \frac{7\tau+4\alpha}{2}} \left(\sum_{i=N_u+1}^{N_t+1} \lambda_i (\nu \tau^{-2} \|\varphi_i\|_0^2 + \|\nabla \varphi_i\|_0^2) + \sum_{i=N_p+1}^{N_t+1} \sigma_i (\nu \|\psi_i\|_0^2 + \|\nabla \psi_i\|_0^2) \right), \end{aligned} \quad (3.26)$$

where the constant $C(\alpha)$ is independent from the discretization and reduced parameters.

Proof. Denote

$$\begin{aligned} \tilde{\mathbf{u}}_r^{n+1} - \tilde{\mathbf{u}}_h^{n+1} &= \tilde{\mathbf{u}}_r^{n+1} - \Pi_{\mathbf{v}} \tilde{\mathbf{u}}_h^{n+1} + \Pi_{\mathbf{v}} \tilde{\mathbf{u}}_h^{n+1} - \tilde{\mathbf{u}}_h^{n+1} := e_{\mathbf{u}}^{n+1} + \theta_{\mathbf{u}}^{n+1}, \\ p_r^{n+1} - p_h^{n+1} &= p_r^{n+1} - \Pi_q p_h^{n+1} + \Pi_q p_h^{n+1} - p_h^{n+1} := e_p^{n+1} + \theta_p^{n+1}. \end{aligned} \quad (3.27)$$

Taking the difference of (2.6) and (3.3) to get

$$\begin{aligned} & (\partial^2 e_{\mathbf{u}}^{n+1}, \mathbf{v}) + (\partial^2 \theta_{\mathbf{u}}^{n+1}, \mathbf{v}) + \nu(\nabla e_{\mathbf{u}}^{n+1}, \nabla \mathbf{v}) + \nu(\nabla \theta_{\mathbf{u}}^{n+1}, \nabla v) \\ & + \frac{1}{3}(\nabla(7e_p^n - 5e_p^{n-1} + e_p^{n-2}), \mathbf{v}) + \frac{1}{3}(\nabla(7\theta_p^n - 5\theta_p^{n-1} + \theta_p^{n-2}), \mathbf{v}) = 0, \end{aligned} \quad (3.28)$$

$$(\nabla \cdot e_{\mathbf{u}}^{n+1}, q) + (\nabla \cdot \theta_{\mathbf{u}}^{n+1}, q) + \frac{2\tau}{3}(\nabla(e_p^{n+1} - e_p^n), \nabla q) + \frac{2\tau}{3}(\nabla(\theta_p^{n+1} - \theta_p^n), \nabla q) = 0. \quad (3.29)$$

Taking $\mathbf{v} = e_{\mathbf{u}}^{n+1}$ and using the equality $2a(3a - 4b + c) = a^2 - b^2 + (2a - b)^2 - (2b - c)^2 + (a - 2b + c)^2$, we have

$$\begin{aligned} & \frac{1}{4\tau}(\|e_{\mathbf{u}}^{n+1}\|_0^2 - \|e_{\mathbf{u}}^n\|_0^2 + \|2e_{\mathbf{u}}^{n+1} - e_{\mathbf{u}}^n\|_0^2 - \|2e_{\mathbf{u}}^n - e_{\mathbf{u}}^{n-1}\|_0^2 + \|e_{\mathbf{u}}^{n+1} - 2e_{\mathbf{u}}^n + e_{\mathbf{u}}^{n-1}\|_0^2) + \nu\|\nabla e_{\mathbf{u}}^{n+1}\|_0^2 \\ & + (\partial^2\theta_{\mathbf{u}}^{n+1}, e_{\mathbf{u}}^{n+1}) + \nu(\nabla\theta_{\mathbf{u}}^{n+1}, \nabla e_{\mathbf{u}}^{n+1}) + \frac{1}{3}(\nabla(7e_p^n - 5e_p^{n-1} + e_p^{n-2}), e_{\mathbf{u}}^{n+1}) \\ & + \frac{1}{3}(\nabla(7\theta_p^n - 5\theta_p^{n-1} + \theta_p^{n-2}), e_{\mathbf{u}}^{n+1}) = 0, \end{aligned}$$

Taking $q = \frac{1}{3}(7e_p^n - 5e_p^{n-1} + e_p^{n-2})$, we obtain

$$\begin{aligned} & -\frac{1}{3}(e_{\mathbf{u}}^{n+1}, \nabla(7e_p^n - 5e_p^{n-1} + e_p^{n-2})) - \frac{1}{3}(\theta_{\mathbf{u}}^{n+1}, \nabla(7e_p^n - 5e_p^{n-1} + e_p^{n-2})) \\ & + \frac{2\tau}{9}(\nabla(e_p^{n+1} - e_p^n), \nabla(7e_p^n - 5e_p^{n-1} + e_p^{n-2})) + \frac{2\tau}{9}(\nabla(\theta_p^{n+1} - \theta_p^n), \nabla(7e_p^n - 5e_p^{n-1} + e_p^{n-2})) = 0. \end{aligned} \quad (3.30)$$

For (3.30) at time t^n and t^{n-1} , we have

$$(\nabla \cdot e_{\mathbf{u}}^n, q) + (\nabla \cdot \theta_{\mathbf{u}}^n, q) + \frac{2\tau}{3}(\nabla(e_p^n - e_p^{n-1}), \nabla q) + \frac{2\tau}{3}(\nabla(\theta_p^n - \theta_p^{n-1}), \nabla q) = 0. \quad (3.31)$$

$$(\nabla \cdot e_{\mathbf{u}}^{n-1}, q) + (\nabla \cdot \theta_{\mathbf{u}}^{n-1}, q) + \frac{2\tau}{3}(\nabla(e_p^{n-1} - e_p^{n-2}), \nabla q) + \frac{2\tau}{3}(\nabla(\theta_p^{n-1} - \theta_p^{n-2}), \nabla q) = 0. \quad (3.32)$$

Subtracting equation (3.30) from equation (3.31) and (3.32)

$$\begin{aligned} & (\nabla \cdot (3e_{\mathbf{u}}^{n+1} - 4e_{\mathbf{u}}^n + e_{\mathbf{u}}^{n-1}), q) + (\nabla \cdot (3\theta_{\mathbf{u}}^{n+1} - 4\theta_{\mathbf{u}}^n + \theta_{\mathbf{u}}^{n-1}), q) \\ & + \frac{2\tau}{3}(\nabla(3e_p^{n+1} - 7e_p^n + 5e_p^{n-1} - e_p^{n-2}), \nabla q) \\ & + \frac{2\tau}{3}(\nabla(3\theta_p^{n+1} - 7\theta_p^n + 5\theta_p^{n-1} - \theta_p^{n-2}), \nabla q) = 0. \end{aligned}$$

and setting $q = e_p^{n+1} - e_p^n$, we obtain

$$\begin{aligned} & (\nabla \cdot (3e_{\mathbf{u}}^{n+1} - 4e_{\mathbf{u}}^n + e_{\mathbf{u}}^{n-1}), e_p^{n+1} - e_p^n) + (\nabla \cdot (3\theta_{\mathbf{u}}^{n+1} - 4\theta_{\mathbf{u}}^n + \theta_{\mathbf{u}}^{n-1}), e_p^{n+1} - e_p^n) \\ & + \frac{2\tau}{3}(\nabla(3e_p^{n+1} - 7e_p^n + 5e_p^{n-1} - e_p^{n-2}), \nabla(e_p^{n+1} - e_p^n)) \end{aligned} \quad (3.33)$$

$$+ \frac{2\tau}{3}(\nabla(3\theta_p^{n+1} - 7\theta_p^n + 5\theta_p^{n-1} - \theta_p^{n-2}), \nabla(e_p^{n+1} - e_p^n)) = 0. \quad (3.34)$$

Adding the all results, the following equality holds

$$\begin{aligned}
& \frac{1}{4\tau}(\|e_{\mathbf{u}}^{n+1}\|_0^2 - \|e_{\mathbf{u}}^n\|_0^2 + \|2e_{\mathbf{u}}^{n+1} - e_{\mathbf{u}}^n\|_0^2 - \|2e_{\mathbf{u}}^n - e_{\mathbf{u}}^{n-1}\|_0^2 + \|e_{\mathbf{u}}^{n+1} - 2e_{\mathbf{u}}^n + e_{\mathbf{u}}^{n-1}\|_0^2) + \nu\|\nabla e_{\mathbf{u}}^{n+1}\|_0^2 \\
& + \frac{\tau}{3}(\|\nabla e_p^{n+1}\|_0^2 - \|\nabla e_p^n\|_0^2 + \|\nabla(e_p^{n+1} - e_p^n)\|_0^2) \\
= & -(\partial^2\theta_{\mathbf{u}}^{n+1}, e_{\mathbf{u}}^{n+1}) - \nu(\nabla\theta_u^{n+1}, \nabla e_u^{n+1}) - \frac{1}{3}(\nabla(7\theta_p^n - 5\theta_p^{n-1} + \theta_p^{n-2}), e_{\mathbf{u}}^{n+1}) \\
& + \frac{1}{3}(\nabla(7e_p^n - 5e_p^{n-1} + e_p^{n-2}), \theta_{\mathbf{u}}^{n+1}) - \frac{2\tau}{9}(\nabla(\theta_p^{n+1} - \theta_p^n), \nabla(7e_p^n - 5e_p^{n-1} + e_p^{n-2})) \\
& + \frac{1}{3}(3e_{\mathbf{u}}^{n+1} - 4e_{\mathbf{u}}^n + e_{\mathbf{u}}^{n-1}, \nabla(e_p^{n+1} - e_p^n)) + \frac{1}{3}(3\theta_{\mathbf{u}}^{n+1} - 4\theta_{\mathbf{u}}^n + \theta_{\mathbf{u}}^{n-1}, \nabla(e_p^{n+1} - e_p^n)) \\
& - \frac{2\tau}{9}(\nabla(e_p^{n+1} - e_p^n), \nabla(3\theta_p^{n+1} - 7\theta_p^n + 5\theta_p^{n-1} - \theta_p^{n-2})) := \sum_{i=1}^8 A_i.
\end{aligned} \tag{3.35}$$

Now we estimate the right hand terms of (3.35). By using the Cauchy-Schwarz inequality, Young inequality, Poincare Inequality and Lemma 3.1, using the spaces $Y = U_r$ and $Z = \text{span}\{\nabla\psi_1, \dots, \nabla\psi_r\}$, we have

$$A_1 \leq \frac{\epsilon_1^{-1}}{4}\|\delta_t\theta_u^{n+1}\|_0^2 + C_p^2\epsilon_1\|\nabla e_u^{n+1}\|_0^2, \tag{3.36}$$

$$A_2 \leq \frac{\epsilon_2^{-1}\nu}{4}\|\nabla\theta_u^{n+1}\|_0^2 + \nu\epsilon_2\|\nabla e_u^{n+1}\|_0^2, \tag{3.37}$$

$$A_3 \leq \frac{\epsilon_3^{-1}}{12}\|7\theta_p^n - 5\theta_p^{n-1} + \theta_p^{n-2}\|_0^2 + \frac{\epsilon_3}{3}\|\nabla e_u^{n+1}\|_0^2, \tag{3.38}$$

$$A_4 \leq \frac{8}{3\tau^2}\|\theta_u^{n+1}\|_0^2 + \tau^2\left(\frac{1}{4}\|\nabla e_p^n\|_0^2 + \frac{1}{3}\|\nabla(e_p^n - e_p^{n-1})\|_0^2 + \frac{1}{12}\|\nabla(e_p^{n-2} - e_p^{n-1})\|_0^2\right), \tag{3.39}$$

$$A_5 \leq \frac{8}{9}\|\nabla(\theta_p^{n+1} - \theta_p^n)\|_0^2 + \frac{\tau^2}{3}\|\nabla e_p^n\|_0^2 + \frac{4\tau^2}{9}\|\nabla(e_p^n - e_p^{n-1})\|_0^2 + \frac{\tau^2}{9}\|\nabla(e_p^{n-2} - e_p^{n-1})\|_0^2, \tag{3.40}$$

$$A_6 \leq \frac{\tau\alpha}{3}\|\partial^2 e_u^{n+1}\|_0^2 + \frac{\tau\alpha}{3}\|\nabla(e_p^n - e_p^{n-1})\|_0^2, \tag{3.41}$$

$$A_7 \leq \frac{1}{3}\|\partial^2\theta_u^{n+1}\|_0^2 + \frac{\tau^2}{3}\|\nabla(e_p^{n+1} - e_p^n)\|_0^2, \tag{3.42}$$

$$A_8 \leq \frac{1}{9}\|\nabla(3\theta_p^{n+1} - 7\theta_p^n + 5\theta_p^{n-1} - \theta_p^{n-2})\|_0^2 + \frac{\tau^2}{9}\|\nabla(e_p^{n+1} - e_p^n)\|_0^2. \tag{3.43}$$

Finally, using the estimates from (3.36) to (3.43), we have

$$\begin{aligned}
& \frac{1}{4\tau} (\|e_{\mathbf{u}}^{n+1}\|_0^2 - \|e_{\mathbf{u}}^n\|_0^2 + \|2e_{\mathbf{u}}^{n+1} - e_{\mathbf{u}}^n\|_0^2 - \|2e_{\mathbf{u}}^n - e_{\mathbf{u}}^{n-1}\|_0^2) + \nu \|\nabla e_{\mathbf{u}}^{n+1}\|_0^2 \\
& + \frac{\tau}{3} (\|\nabla e_p^{n+1}\|_0^2 - \|\nabla e_p^n\|_0^2 + \|\nabla(e_p^{n+1} - e_p^n)\|_0^2) \leq \\
& \left(\frac{\epsilon_1^{-1}}{4} + \frac{1}{3} \right) \|\partial^2 \theta_u^{n+1}\|_0^2 + \frac{\epsilon_2^{-1} \nu}{4} \|\nabla \theta_u^{n+1}\|_0^2 + (C_p^2 \epsilon_1 + \nu \epsilon_2 + \frac{\epsilon_3}{3}) \|\nabla e_u^{n+1}\|_0^2 + \frac{\epsilon_3^{-1}}{12} \|7\theta_p^n - 5\theta_p^{n-1} + \theta_p^{n-2}\|_0^2 \\
& + \frac{8}{3\tau^2} \|\theta_u^{n+1}\|_0^2 + \left(\frac{\tau^2}{4} + \frac{\tau^2}{3} \right) \|\nabla e_p^n\|_0^2 + \left(\frac{\tau^2}{3} + \frac{4\tau^2}{9} \right) \|\nabla(e_p^n - e_p^{n-1})\|_0^2 + \left(\frac{\tau^2}{12} + \frac{\tau^2}{9} \right) \|\nabla(e_p^{n-2} - e_p^{n-1})\|_0^2 \\
& + \frac{\tau\alpha}{3} \|\partial^2 e_u^{n+1}\|_0^2 + \left(\frac{\tau\alpha + \tau^2}{3} + \frac{\tau^2}{9} \right) \|\nabla(e_p^{n+1} - e_p^n)\|_0^2 + \frac{8}{9} \|\nabla(\theta_p^{n+1} - \theta_p^n)\|_0^2 \\
& + \frac{1}{9} \|\nabla(3\theta_p^{n+1} - 7\theta_p^n + 5\theta_p^{n-1} - \theta_p^{n-2})\|_0^2. \tag{3.44}
\end{aligned}$$

Taking in (3.44) $\epsilon_1 = \frac{\nu}{6C_p^2}$, $\epsilon_2 = \frac{1}{6}$ and $\epsilon_3 = \frac{\nu}{2}$ and multiplying by 4τ , we obtain:

$$\begin{aligned}
& \|e_{\mathbf{u}}^{n+1}\|_0^2 - \|e_{\mathbf{u}}^n\|_0^2 + \|2e_{\mathbf{u}}^{n+1} - e_{\mathbf{u}}^n\|_0^2 - \|2e_{\mathbf{u}}^n - e_{\mathbf{u}}^{n-1}\|_0^2 + \|e_u^{n+1} - 2e_u^n + e_u^{n-1}\|_0^2 \\
& + \frac{4\tau\nu}{2} \|\nabla e_{\mathbf{u}}^{n+1}\|_0^2 + \frac{4\tau^2}{3} (\|\nabla e_p^{n+1}\|_0^2 - \|\nabla e_p^n\|_0^2 + \|\nabla(e_p^{n+1} - e_p^n)\|_0^2) \leq \\
& 4\tau \left(\frac{6C_p^2}{4\nu} + \frac{1}{3} \right) \|\partial^2 \theta_u^{n+1}\|_0^2 + \frac{4\tau\nu}{24} \|\nabla \theta_u^{n+1}\|_0^2 + \frac{4\tau\nu}{24} \|7\theta_p^n - 5\theta_p^{n-1} + \theta_p^{n-2}\|_0^2 \\
& + \frac{32}{3\tau} \|\theta_u^{n+1}\|_0^2 + 4\tau \left(\frac{\tau^2}{4} + \frac{\tau^2}{3} \right) \|\nabla e_p^n\|_0^2 + 4\tau \left(\frac{\tau^2}{3} + \frac{4\tau^2}{9} \right) \|\nabla(e_p^n - e_p^{n-1})\|_0^2 \\
& + 4\tau \left(\frac{\tau^2}{12} + \frac{\tau^2}{9} \right) \|\nabla(e_p^{n-2} - e_p^{n-1})\|_0^2 + 4\tau \left(\frac{\tau\alpha + \tau^2}{3} + \frac{\tau^2}{9} \right) \|\nabla(e_p^{n+1} - e_p^n)\|_0^2 \\
& + 4\tau \frac{8}{9} \|\nabla(\theta_p^{n+1} - \theta_p^n)\|_0^2 + \frac{4\tau}{9} \|\nabla(3\theta_p^{n+1} - 7\theta_p^n + 5\theta_p^{n-1} - \theta_p^{n-2})\|_0^2 + \frac{4\tau^2\alpha}{3} \|\partial^2 e_u^{n+1}\|_0^2. \tag{3.45}
\end{aligned}$$

Summing (3.45) from $n = 1$ to $k < N_t$ and following the same procedure as in Lemma 3 of [5], we have:

$$\begin{aligned}
& \|e_u^{k+1}\| + \frac{4\tau\nu}{2} \sum_{n=1}^k \|\nabla e_u^{n+1}\|_0^2 + \frac{4\tau^2}{3} \|\nabla e_p^{k+1}\| + \frac{4\tau^2(1 - \frac{17\tau}{4} - \alpha)}{3} \|\nabla(e_p^{n+1} - e_p^n)\|_0^2 \leq \\
& 7\|e_u^1\|_0^2 + 3\|e_u^0\|_0^2 + \frac{4\tau^2}{3} \|\nabla e_p^1\|_0^2 + 4\tau \left(\frac{\tau^2}{4} + \frac{\tau^2}{3} \right) \sum_{n=1}^k \|\nabla e_p^n\|_0^2 + \frac{4\tau^2\alpha}{3} \sum_{n=1}^k \|\partial^2 e_u^{n+1}\|_0^2 \\
& + 4 \left(\frac{6C_p^2}{4\nu} + \frac{1}{3} \right) \sum_{n=1}^k \tau \|\partial^2 \theta_u^{n+1}\|_0^2 + \frac{4\nu}{24} \sum_{n=1}^k \tau \|\nabla \theta_u^{n+1}\|_0^2 + \frac{4\nu}{24} \sum_{n=1}^k \tau \|7\theta_p^n - 5\theta_p^{n-1} + \theta_p^{n-2}\|_0^2 \\
& + \frac{32}{3\tau^2} \sum_{n=1}^k \tau \|\theta_u^{n+1}\|_0^2 + \frac{32}{9} \sum_{n=1}^k \tau \|\nabla(\theta_p^{n+1} - \theta_p^n)\|_0^2 + \frac{4}{9} \sum_{n=1}^k \tau \|\nabla(3\theta_p^{n+1} - 7\theta_p^n + 5\theta_p^{n-1} - \theta_p^{n-2})\|_0^2. \tag{3.46}
\end{aligned}$$

Bounding the temporal derivate of the error. We estimate the time derivative of the error using the same idea as in [4, Theorem 2]. First, we consider $\mathbf{v} = \partial^2 e_{\mathbf{u}}^{n+1}$ in (3.28):

$$\begin{aligned} & \|\partial^2 e_{\mathbf{u}}^{n+1}\|_0^2 + (\partial^2 \theta_{\mathbf{u}}^{n+1}, \partial^2 e_{\mathbf{u}}^{n+1}) + \nu(\nabla e_{\mathbf{u}}^{n+1}, \nabla \partial^2 e_{\mathbf{u}}^{n+1}) + \nu(\nabla \theta_{\mathbf{u}}^{n+1}, \partial^2 e_{\mathbf{u}}^{n+1}) \\ & + \frac{1}{3}(\nabla(7e_p^n - 5e_p^{n-1} + e_p^{n-2}), \partial^2 e_{\mathbf{u}}^{n+1}) + \frac{1}{3}(\nabla(7\theta_p^n - 5\theta_p^{n-1} + \theta_p^{n-2}), \partial^2 e_{\mathbf{u}}^{n+1}) = 0, \end{aligned} \quad (3.47)$$

Then, by using the same equality as in (3.30) we obtain:

$$\begin{aligned} 4\tau \|\partial^2 e_{\mathbf{u}}^{n+1}\|_0^2 + \nu \|\nabla e_{\mathbf{u}}^{n+1}\|_0^2 + \nu \|\nabla(2e_{\mathbf{u}}^{n+1} - e_{\mathbf{u}}^n)\|_0^2 + \nu \|\nabla(e_{\mathbf{u}}^{n+1} - 2e_{\mathbf{u}}^n + e_{\mathbf{u}}^{n-1})\|_0^2 = \\ \nu \|\nabla e_{\mathbf{u}}^n\|_0^2 + \nu \|\nabla(2e_{\mathbf{u}}^n - e_{\mathbf{u}}^{n-1})\|_0^2 + 4\tau(A, \partial^2 e_{\mathbf{u}}^{n+1}), \end{aligned} \quad (3.48)$$

where

$$(A, \partial^2 e_{\mathbf{u}}^{n+1}) = (-\partial^2 \theta_{\mathbf{u}}^{n+1} - \nu \theta_{\mathbf{u}}^{n+1} - \frac{1}{3} \nabla(7e_p^n - 5e_p^{n-1} + e_p^{n-2}) - \frac{1}{3} \nabla(7\theta_p^n - 5\theta_p^{n-1} + \theta_p^{n-2}), \partial^2 e_{\mathbf{u}}^{n+1}).$$

Now, by applying the Cauchy-Schwarz inequality and Young Inequality in (3.48):

$$\begin{aligned} 2\tau \|\partial^2 e_{\mathbf{u}}^{n+1}\|_0^2 + \nu \|\nabla e_{\mathbf{u}}^{n+1}\|_0^2 + \nu \|\nabla(2e_{\mathbf{u}}^{n+1} - e_{\mathbf{u}}^n)\|_0^2 + \nu \|\nabla(e_{\mathbf{u}}^{n+1} - 2e_{\mathbf{u}}^n + e_{\mathbf{u}}^{n-1})\|_0^2 \leq \\ \nu \|\nabla e_{\mathbf{u}}^n\|_0^2 + \nu \|\nabla(2e_{\mathbf{u}}^n - e_{\mathbf{u}}^{n-1})\|_0^2 + 2\tau \|A\|_0^2. \end{aligned} \quad (3.49)$$

Therefore, summing from $n = 1$ to $k < N_t$ in (3.49) and simplifying, using the same procedure as in Lemma 3 of [5]:

$$\sum_{n=1}^k 2\tau \|\partial^2 e_{\mathbf{u}}^{n+1}\|_0^2 \leq \nu(7\|\nabla e_{\mathbf{u}}^1\|_0^2 + 3\|\nabla e_{\mathbf{u}}^0\|_0^2) + \sum_{n=1}^k 2\tau \|A\|_0^2. \quad (3.50)$$

Once the temporal derivative of the error is bounded, using the following estimate:

$$\begin{aligned} \tau \|A\|_0^2 \leq \tau \|\partial^2 \theta_{\mathbf{u}}^{n+1}\|_0^2 + \tau \nu \|\nabla \theta_{\mathbf{u}}^{n+1}\|_0^2 + \tau \|\nabla e_p^n\|_0^2 + \frac{4\tau}{3} \|\nabla(e_p^n - e_p^{n-1})\|_0^2 + \\ \frac{\tau}{3} \|\nabla(e_p^{n-1} - e_p^{n-2})\|_0^2 + \frac{\tau}{3} \|\nabla(7\theta_p^n - 5\theta_p^{n-1} + \theta_p^{n-2})\|_0^2, \end{aligned}$$

and introduce (3.50) into (3.46), assuming that $\tau < \frac{4(1 - \frac{8}{3}\alpha)}{17}$:

$$\begin{aligned} \|e_u^{k+1}\| + \frac{4\tau\nu}{2} \sum_{n=1}^k \|\nabla e_u^{n+1}\|_0^2 + \frac{4\tau^2}{3} \|\nabla e_p^{k+1}\| \leq 7\|e_u^1\|_0^2 + 3\|e_u^0\|_0^2 + \frac{4\tau^2}{3} \|\nabla e_p^1\|_0^2 \\ + \frac{2\nu\tau\alpha}{3} (7\|\nabla e_u^1\|_0^2 + 3\|\nabla e_u^0\|_0^2) + 4\tau \left(\frac{\tau^2}{4} + \frac{\tau^2}{3} + \frac{\tau\alpha}{3} \right) \sum_{n=1}^k \|\nabla e_p^n\|_0^2 + 4 \left(\frac{6C_p^2}{4\nu} + \frac{1}{3} + \frac{\tau\alpha}{3} \right) \sum_{n=1}^k \tau \|\partial^2 \theta_u^{n+1}\|_0^2 \\ + \frac{4\nu(1 + \frac{\tau\alpha}{3})}{24} \sum_{n=1}^k \tau \|\nabla \theta_u^{n+1}\|_0^2 + \frac{4\nu}{24} \sum_{n=1}^k \tau \|7\theta_p^n - 5\theta_p^{n-1} + \theta_p^{n-2}\|_0^2 + \frac{32}{3\tau^2} \sum_{n=1}^k \tau \|\theta_u^{n+1}\|_0^2 \\ + \frac{32}{9} \sum_{n=1}^k \tau \|\nabla(\theta_p^{n+1} - \theta_p^n)\|_0^2 + \left(\frac{4}{9} + \frac{4\tau\alpha}{9} \right) \sum_{n=1}^k \tau \|\nabla(3\theta_p^{n+1} - 7\theta_p^n + 5\theta_p^{n-1} - \theta_p^{n-2})\|_0^2 = 7\|e_u^1\|_0^2 + 3\|e_u^0\|_0^2 \\ + \frac{4\tau^2}{3} \|\nabla e_p^1\|_0^2 + \frac{2\nu\tau\alpha}{3} (7\|\nabla e_u^1\|_0^2 + 3\|\nabla e_u^0\|_0^2) + \frac{7\tau + 4\alpha}{4} \sum_{n=1}^k \frac{4\tau^2}{3} \|\nabla e_p^n\|_0^2 + \sum_{i=1}^6 B_i. \end{aligned} \quad (3.51)$$

Now, by applying Gronwall's lemma (see for instance [11], Lemma 5.1) in (3.46) we get:

$$\begin{aligned} & \max_{1 \leq k \leq N+1} \|e_u^k\|_0^2 + \frac{4\tau\nu}{2} \sum_{n=1}^N \|\nabla e_u^{n+1}\|_0^2 + \max_{1 \leq k \leq N+1} \frac{4\tau^2}{3} \|\nabla e_p^k\|_0^2 \\ & \leq e^{\frac{7\tau+4\alpha}{2}T} (7\|e_u^1\|_0^2 + 3\|e_u^0\|_0^2 + C(\nu, \alpha)(7\|\nabla e_u^1\|_0^2 + 3\|\nabla e_u^0\|_0^2) + \frac{4\tau^2}{3} \|\nabla e_p^1\|_0^2 + 2 \sum_{i=1}^6 B_i^N). \end{aligned} \quad (3.52)$$

Therefore, using POD projection error estimates, we can bound the terms $\{B_i^N\}_{i=1}^6$ on the right-hand side of (3.52) obtaining:

$$\begin{aligned} & \max_{1 \leq k \leq N_t+1} \|e_u^k\|_0^2 + \frac{4\tau\nu}{2} \sum_{n=1}^{N_t} \|\nabla e_u^{n+1}\|_0^2 + \max_{1 \leq k \leq N_t+1} \frac{4\tau^2}{3} \|\nabla e_p^k\|_0^2 \\ & \leq e^{\frac{7\tau+4\alpha}{2}T} (7\|e_u^1\|_0^2 + 3\|e_u^0\|_0^2 + \frac{4\tau^2}{3} \|\nabla e_p^1\|_0^2 + C(\nu, \alpha)(7\|\nabla e_u^1\|_0^2 + 3\|\nabla e_u^0\|_0^2) + \\ & C(\alpha) \left(\sum_{i=N_u+1}^{M_u} \lambda_i (\alpha\nu\tau^{-2} \|\varphi_i\|_0^2 + \|\nabla\varphi_i\|_0^2) + \sum_{i=N_p+1}^{M_p} \sigma_i (\nu\|\psi_i\|_0^2 + \|\nabla\psi_i\|_0^2) \right)). \end{aligned} \quad (3.53)$$

Finally, taking the ROM initial conditions as the POD projection of the FOM initial solutions, then (3.53) reads:

$$\begin{aligned} & \max_{1 \leq k \leq N_t+1} \|e_u^k\|_0^2 + \frac{4\tau\nu}{2} \sum_{n=1}^{N_t} \|\nabla e_u^{n+1}\|_0^2 + \max_{1 \leq k \leq N_t+1} \frac{4\tau^2}{3} \|\nabla e_p^k\|_0^2 \\ & \leq C(\alpha) e^{\frac{7\tau+4\alpha}{2}T} \left(\sum_{i=N_u+1}^{M_u} \lambda_i (\nu\tau^{-2} \|\varphi_i\|_0^2 + \|\nabla\varphi_i\|_0^2) + \sum_{i=N_p+1}^{M_p} \sigma_i (\nu\|\psi_i\|_0^2 + \|\nabla\psi_i\|_0^2) \right). \end{aligned} \quad (3.54)$$

Finally, using the following inequality:

$$\begin{aligned} & \sum_{n=1}^{N_t} \tau \|e_u^{n+1}\|^2 \leq T \max_{1 \leq k \leq N_t} \|e_u^{k+1}\|^2, \\ & \sum_{n=1}^{N_t} \tau \|e_p^{n+1}\|^2 \leq T \max_{1 \leq k \leq N_t} \|e_p^{k+1}\|^2, \end{aligned} \quad (3.55)$$

the triangle inequality, we reach the error bound (3.26). \square

Remark 3.2. *We can note that we have a factor of τ^2 in front of the pressure term in the stability (3.6) and the POD truncation error estimation (3.26), this can be avoid as in [1].*

4. THE NUMERICAL RESULTS

In this section, we present some numerical results for the BDF2 time-splitting scheme introduced and analyzed in the previous section. In order to evaluate the accuracy of the ROM, we show two numerical experiments with Dirichlet boundary conditions.

First, we verify the precision of the numerical scheme by using a solution with relatively high regularity. Then, we have consider this solution in order to generate the snapshots to construct the corresponding reduced order model, and analyze its behaviour with different numbers of POD modes. Finally, we demonstrate some reliable results through a classic benchmark text, i.e. lid driven cavity flow.

4.1. Accuracy Test. The accuracy test comming from a preescribed solution given by [15]:

$$\begin{cases} u(x, y, t) &= \cos(t)\pi \sin(\pi x)^2 \sin(2\pi y), \\ v(x, y, t) &= \cos(t)\pi \sin(\pi x)^2 \sin(2\pi y), \\ p(x, y, t) &= 10 \cos(t) \cos(\pi x) \cos(\pi y). \end{cases} \quad (4.1)$$

We have consider $\Omega = [0, 1] \times [0, 1] \subset \mathbb{R}^2$ as computational domain, the time interval is $[0, T]$, where $T = 1$, and the viscosity coefficient is $\nu = 1$. The numerical method used for solving the problem is the one described in Section (2.2), moreover the spatial discretization used is $\mathbb{P}^2 - \mathbb{P}^1$ for the pair velocity-pressure on a relatively coarse computational grid, for which we consider a uniform partition of the cavity on 100^2 cells. In table (1) we present the L^2 error between the exact solution and the FE solution with different time step size in order to demonstrate the second-order of the scheme. The table also display the convergences rates, confirming that the suggested scheme achieved the desired accuracy.

TABLE 1. Time convergence of scheme for Stokes problem with the exact solution (4.1).

τ	$\ u_{exact} - u_h\ _{L^2}$	Rate	$\ p_{exact} - p_h\ _{L^2}$	Rate
1/20	3.09e-02		4.27e-01	
1/40	8.42e-03	1.8793	1.20e-01	1.8300
1/80	2.14e-03	1.9712	3.11e-02	1.9459
1/160	5.40e-04	1.9917	7.89e-03	1.9812

4.1.1. POD Reduced Order Model. Now, we will demonstrate the effectiveness and efficiency of the ROM described in Section (3) for the Stokes problem with the exact solution described above. The numerical method to get the snapshots is the before one, using $\tau = 10^{-2}$ in the FOM simulations. For the ROM, we collect $M = 81$ snapshots for each unknown field, by storing every fourth FOM simulations in the time interval $[0.21, 1]$, in order to avoid numerical inestabilities at the beginning of the simulation. The POD modes are generated in L^2 -norm for velocity and pressure. In the following, we will analyze the discrete relative error between the FE solution s_h and the ROM solution s_r in the $l^2(L^2)$ -norm, defined as:

$$\frac{\|s_h - s_r\|_{l^2(L^2)}}{\|s_h\|_{l^2(L^2)}} = \sqrt{\frac{\sum_{i=1}^M \|s_h^i - s_r^i\|_0^2}{\sum_{i=1}^M \|s_h^i\|_0^2}}$$

The decay of POD eigenvalues (left) and captured energy (right) computed by $100 \sum_{k=1}^r \lambda_k / \sum_{k=1}^M \lambda_k$, where λ_k are the corresponding eigenvalues and M the rank of the corresponding data set of the problem of each field are shown in Figure (1). Note that the maximum dimension of the reduced space is 3 for the velocity field and 5 for the pressure field. This is because the decay of the eigenvalues stabilizes beyond these values, and, consequently, the subsequent eigenfunctions are not linearly independent. In Figure (2), we show the $l^2(L^2)$ relative errors for both velocity (left) and pressure (right). For

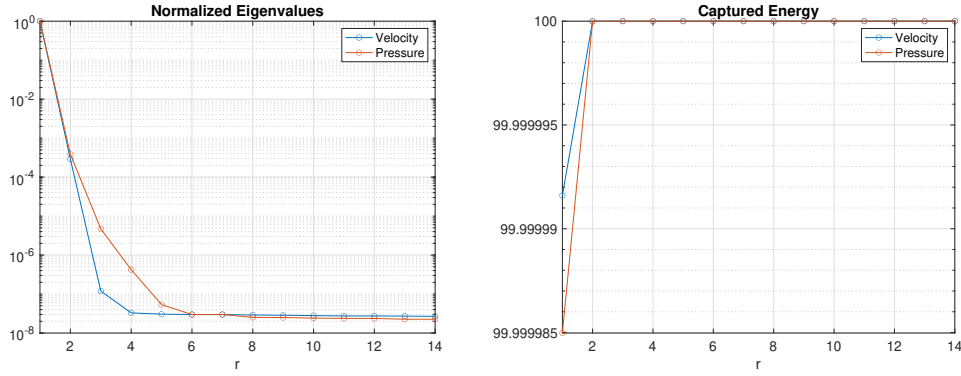


FIGURE 1. Decay of the normalized POD eigenvalues (left) and captured energy (right).

comparison purposes, we also plot the $l^2(L^2)$ relative projection errors for both velocity and pressure in the same figure. It is worth noting that this error represents the best achievable error.

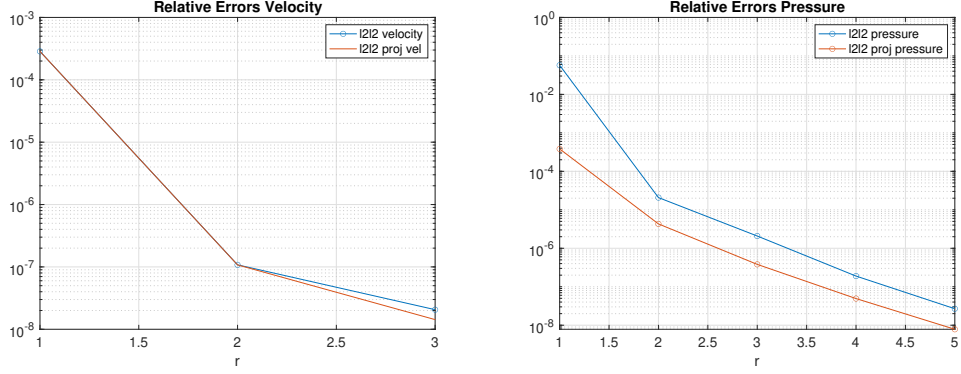


FIGURE 2. l^2l^2 errors of velocity and pressure.

We can also observe in Figure (2) that for the velocity case, using 2 basis functions results in negligible relative errors on the order of 10^{-7} . However, due to the slower decay of pressure eigenvalues with respect to the velocity ones, as we can see in Figure (1), to achieve the same order of error for the pressure, 4 basis functions are required.

Finally, Figure 3 shows a comparison between the theoretical error estimator (3.26) and the velocity and error pressure error depending on the number of modes (r).

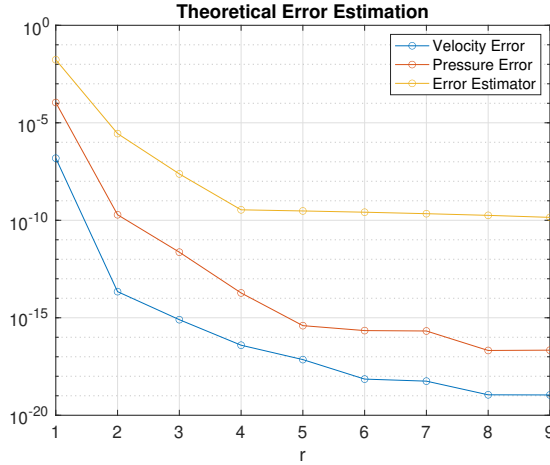


FIGURE 3. Comparative between the theoretical error estimator (3.26) and the velocity and pressure error depending on the number of modes (r).

4.2. Lid-driven cavity flow. The lid-driven cavity problem is a classical benchmark in computational fluid dynamics, widely studied for its rich flow structures and well-defined boundary conditions. This problem involves a square or rectangular domain where the fluid is driven by the motion of the upper boundary (lid) while the remaining walls remain stationary. In this work, we focus on a specific configuration where Dirichlet boundary conditions are imposed: the lid has a prescribed tangential velocity, and the side and bottom walls enforce no-slip conditions. Additionally, the right-hand side term in the governing equations is set to zero, i.e., $f = 0$. corresponding to the absence of external forces.

Through numerical simulation, we analyze the velocity and pressure fields, highlighting the accuracy and stability of our method. The lid-driven cavity setup provides an excellent test case for evaluating the performance of numerical schemes, given its well-documented solutions and the presence of flow features such as vortices and shear layers.

For this test, we have considered, as mentioned above, $\Omega = [0, 1] \times [0, 1]$ as computational domain. Additionally, for the ROM, both time and Reynolds number have been considered as parameters, resulting in a multiparametric ROM. The Reynolds number lies within the range $\mathcal{D} = [1000, 5000]$, where all solutions reach a steady-state regime.

4.2.1. Snapshots Generation for POD construction. The numerical method used for solving the problem is the one described in Section (3), moreover the spatial discretization used is $\mathbb{P}^2 - \mathbb{P}^1$ FE for the pair velocity-pressure on a mesh that is refined towards the walls in both directions to accurately capture the unknown fields, using the hyperbolic tangent function: [10, 16]:

$$f(x) = 0.5 \left(1 + \frac{\tanh(2(2x - 1))}{\tanh(2)} \right). \quad (4.2)$$

We have considered a cavity with a partition of 64^2 .

In the FOM simulations, an impulsive start is applied, with initial conditions set to zero for both velocity and pressure fields. The time step used is $\Delta t = 5 \cdot 10^{-3}$. Time integration is carried

out using the incremental projection detailed in Section (2.2). To handle the convection non-linear Navier–Stokes term $(\tilde{u} \cdot \nabla)\tilde{u}$ which appears in the momentum equation, we have considered the following extrapolation by means of Newton–Gregory backward polynomials ([2]) : $((2\tilde{u}^n - \tilde{u}^{n-1}) \cdot \nabla)\tilde{u}^{n+1}$, $n \geq 1$, in order to achieve a second-order accuracy in time.

We have considered a multiparametric ROM, as mentioned above, considering a physical parameter, Reynolds number Re , and the time t . For the physical parameter we take 5 sample in a uniformly partition of the range $\mathcal{D} = [1000, 5000]$. For the time variable, although we have considered solutions that reach a steady-state regime, we have taken the solution in the interval $[2, 3]$, where the steady-state has not yet been achieved. Finally, we have collect $M = 200 \cdot 5 = 1000$ snapshots for each unknown field. The POD modes are generated using L^2 –norm for both velocity and pressure. To determine the dimension of the reduced space, Figure (4) illustrates the decay of the eigenvalues (left) and the captured energy (right). From Figure (4), we can observe that with 4 modes, more than 99% of the energy is captured for both velocity and pressure.

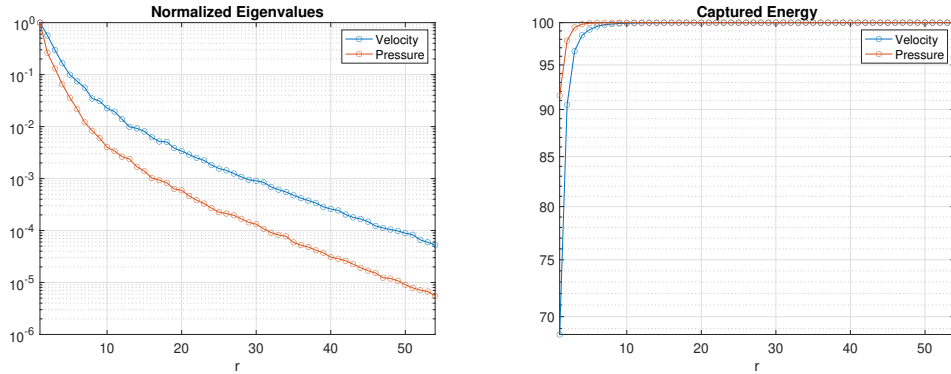


FIGURE 4. Decay of the normalized POD eigenvalues (left) and captured energy (right).

4.2.2. Numerical Results. Once the POD modes are generated, the ROM is constructed by using the same time discretization as the FOM. We have evaluated the ROM in the same time interval as its constructed, for different physical parameters values and also, for extrapolation in time.

Figure (5) shows the $l^2(L^2)$ relative errors for both velocity (left) and pressure (right) for two different values of our physical parameter set, adding the $l^2(L^2)$ relative projection errors because this represent the best achievable error.

We can see in Figure (5) that the $l^2(L^2)$ error exhibits the same behavior as its projection error, achieving very small errors with only a few modes.

We also evaluate the performance of the ROM with respect to extrapolation in time. Using two samples of the Reynolds parameter ($Re \in \{2000, 4000\}$), we analyze the ROM over the time interval $(2, 4]$, while snapshots are collected in the time interval $(2, 3]$. To assess the ROM's performance in this scenario, Figure 8 depicts the temporal evolution of the L^2 error in space for velocity (left) and pressure (right).

At the same time, to evaluate the performance of the ROM with respect interpolation for the physical parameter, we select different values from the samples inside the range $\mathcal{D} = [1000, 5000]$.

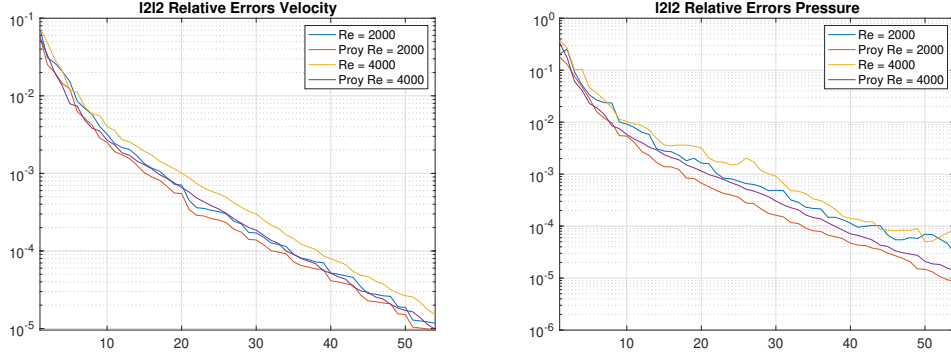
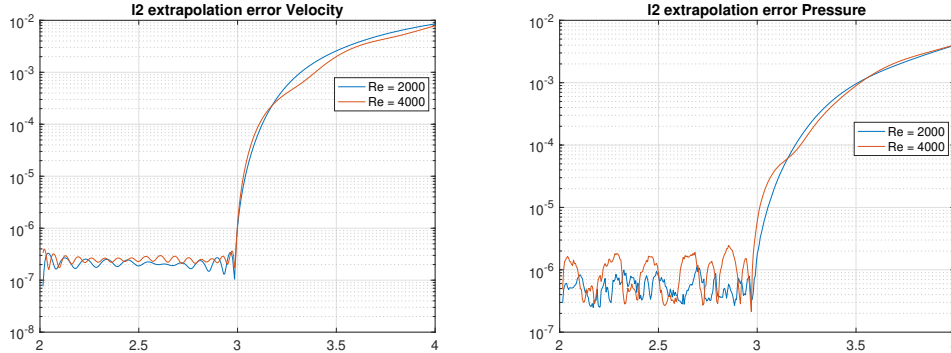
FIGURE 5. $l2l2$ errors of velocity and pressure.FIGURE 6. $l2$ error extrapolation time

Figure (7) show the $l^2(L^2)$ relative error of velocity and pressure computing in the same time interval as snapshots, [2, 3].

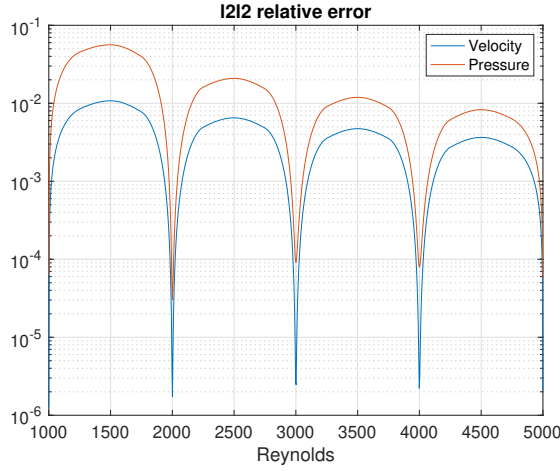
In Figure (7), We can see that the maximum error for both velocity and pressure takes at the mean value between each sample of the physical parameter, with the highest errors obtained for $Re = 1500$.

5. CONCLUSION

In this work, we have proposed a reduced-order model (ROM) for the incompressible Navier–Stokes equations based on an incremental projection scheme combined with Proper Orthogonal Decomposition (POD) techniques. The model employs BDF2 time discretization and finite element spatial approximation, achieving second-order accuracy in time.

The reduced scheme effectively decouples velocity and pressure computations, while preserving stability and bypassing the inf-sup condition via a stabilized pressure formulation. We provided a detailed stability analysis and established error estimates, demonstrating that the velocity error in the semi-discrete norm is of order $\mathcal{O}(\delta t^2 + h^{l+1})$, and the splitting error remains of order $\mathcal{O}(\delta t^2)$.

Numerical results validate the theoretical analysis. The benchmark Stokes problem confirmed the expected second-order convergence in time. In the POD-ROM simulations, very few modes were

FIGURE 7. l_2l_2 relative error parameter extrapolation

sufficient to attain high accuracy; for instance, negligible relative errors ($\sim 10^{-7}$) were achieved using only two velocity modes.

The classical lid-driven cavity problem served as a further benchmark to evaluate the ROM under multiparametric conditions, including variations in Reynolds number and time. The ROM successfully captured key flow features, demonstrating both accuracy and computational efficiency, even when extrapolating in time and interpolating in parameter space.

Overall, this framework presents a promising approach for reduced-order modeling of incompressible flows. Future research will focus on extending the method to the full nonlinear Navier–Stokes equations, adaptive mode selection strategies, and integration with data-driven or machine learning approaches to enhance ROM capabilities in more complex settings.

Acknowledgments: This work has been supported by the Spanish Government Project PID2021-123153OBC21. The research of M. Azaiez has been supported by “Visiting Scholars” du “VII Plan Propio de Investigación y Transferencia” of the University of Seville (Spain) and the French National Research Agency ANR-22-CE46-0005 (NumOPT)

REFERENCES

- [1] M. Azañez, T. Chacón Rebollo, C. Núñez Fernández, and S. Rubino. A pod-based reduced order method applied to goda time-splitting scheme. *Journal of Scientific Computing*, 104(1):9, 2025.
- [2] François E. Cellier. *Continuous system modeling*. New York etc.: Springer-Verlag, 1991.
- [3] A.J. Chorin. Numerical solution of the navier–stokes equations. *Math. Comput.*, 22(4):745–762, 1968.
- [4] Bosco García-Archilla, V. John, and Julia Novo. Error analysis of BDF schemes for the evolutionary incompressible Navier–Stokes equations. Preprint, arXiv:2506.16917 [math.NA] (2025), 2025.
- [5] Bosco García-Archilla, Volker John, and Julia Novo. Second order error bounds for POD-ROM methods based on first order divided differences. *Appl. Math. Lett.*, 146:7, 2023. Id/No 108836.
- [6] R. Glowinski. *Finite element methods for incompressible viscous flow*. Elsevier Science B.V., Amsterdam, 2003.
- [7] Katuhiko Goda. A multistep technique with implicit difference schemes for calculating two- or three-dimensional cavity flows. *J. Comput. Phys.*, 30:76–95, 1979.
- [8] J-L Guermond and Abner J Salgado. Error analysis of a fractional time-stepping technique for incompressible flows with variable density. *SIAM Journal on Numerical Analysis*, 49(3):917–944, 2011.
- [9] Jean-Luc Guermond, Peter Minev, and Jie Shen. An overview of projection methods for incompressible flows. *Computer methods in applied mechanics and engineering*, 195(44-47):6011–6045, 2006.
- [10] Ryadh Haferssas, Pierre Jolivet, and Samuele Rubino. Efficient and scalable discretization of the Navier-Stokes equations with LPS modeling. *Comput. Methods Appl. Mech. Eng.*, 333:371–394, 2018.
- [11] John G. Heywood and Rolf Rannacher. Finite-element approximation of the nonstationary Navier-Stokes problem. IV: Error analysis for second-order time discretization. *SIAM J. Numer. Anal.*, 27(2):353–384, 1990.
- [12] Guermond Jean-Luc. A convergence result for the approximation of the navier-stokes equations by an incremental projection method. *C. R. Acad. Sci. Paris, Série I*, 325(12):1329–1332, 1997.
- [13] K. Kunisch and S. Volkwein. Galerkin proper orthogonal decomposition methods for parabolic problems. *Numer. math.*, 90(1):117–148, 2001.
- [14] Xi Li, Yan Luo, and Minfu Feng. An efficient Chorin-Temam projection proper orthogonal decomposition based reduced-order model for nonstationary Stokes equations. *J. Sci. Comput.*, 93(3):26, 2022. Id/No 64.
- [15] Xi Li, Yan Luo, and Minfu Feng. An efficient chorin-temam projection proper orthogonal decomposition based reduced-order model for nonstationary stokes equations. *Journal of Scientific Computing*, 93(3):64, 2022.
- [16] Samuele Rubino. An efficient time-splitting approximation of the Navier-Stokes equations with LPS modeling. *Appl. Math. Comput.*, 348:318–337, 2019.
- [17] Samuele Rubino. Numerical analysis of a projection-based stabilized POD-ROM for incompressible flows. *SIAM J. Numer. Anal.*, 58(4):2019–2058, 2020.
- [18] R. Temam. Sur l'approximation de la solution des équations de navier–stokes par la méthode des pas fractionnaires ii. *MArch. Ration. Mech. Anal.*, 33(4):377–385, 1969.
- [19] N.N. Yanenko. *The Method of Fractional Steps. The Solution of Problems of Mathematical Physics in Several Variables*. Springer-Verlag, New York, 1971.